

## Long-Range Nonlocal Flow of Vortices in Narrow Superconducting Channels

I. V. Grigorieva, A. K. Geim, S. V. Dubonos, and K. S. Novoselov

*Department of Physics and Astronomy, University of Manchester, Oxford Road, Manchester M13 9PL, United Kingdom*

D. Y. Vodolazov and F. M. Peeters

*Departement Natuurkunde, Universiteit Antwerpen, Universiteitsplein 1, B-2610 Antwerpen, Belgium*

P. H. Kes and M. Hesselberth

*Kamerlingh Onnes Laboratorium, Leiden University, P.O. Box 9504, 2300 RA Leiden, The Netherlands*

(Received 1 December 2003; published 8 June 2004)

We report a new nonlocal effect in vortex matter, where an electric current confined to a small region of a long and sufficiently narrow superconducting wire causes vortex flow at distances hundreds of intervortex separations away. The observed remote traffic of vortices is attributed to a very efficient transfer of a local strain through the one-dimensional vortex lattice (VL), even in the presence of disorder. We also observe mesoscopic fluctuations in the nonlocal vortex flow, which arise due to “traffic jams” when vortex arrangements do not match a local geometry of a superconducting channel.

DOI: 10.1103/PhysRevLett.92.237001

PACS numbers: 74.25.Qt, 73.23.-b, 74.20.-z, 74.78.-w

Phenomena associated with vortex motion in superconductors have been subject to intense interest for many decades, as they are important both for applications and in terms of interesting, complex physics involved. Vortices start moving when the Lorentz force  $f_L$  acting on them exceeds pinning forces arising from always-present defects. The force is determined by the local current density  $j$  and, hence, the resulting vortex motion is confined essentially to the region where the applied current flows [1,2]. There are only a few cases known where vortex flow becomes nonlocal (i.e., not limited to the current region), most notably in Giaever’s flux transformer [3] and in layered superconductors [4]. In the former case,  $f_L$  is applied to vortices in one of the superconducting films comprising the transformer, while the voltage is generated in the second film, due to electromagnetic coupling between vortices in the two films [3,5]. In layered superconductors, a drag effect (somewhat similar to that in Giaever’s transformer) is observed due to coupling between pancake vortices in different layers. Both nonlocal effects occur along vortices and are basically due to their finite rigidity. A high viscosity of a vortex matter can also lead to a nonlocal response in the direction *perpendicular* to vortices [6–9]. In this case, local vortex displacements induced by  $j$  create secondary forces on their neighbors pushing them along. Such nonlocal correlations were observed in the vicinity of the melting transition in high-temperature superconductors [8,9]. This is a dynamic effect where VLs regions—generally moving at different speeds due to different above-critical currents—suddenly become locked in a long-range collective motion. In the absence of a driving current, such viscosity-induced nonlocality is expected to die off at a few vortex separations [6,7].

In this Letter, we report a nonlocal effect of a different kind, which arises *in the absence of a driving current* due

to a long-range collective response of a rigid one-dimensional (1D) VL and survives at strikingly long distances, corresponding to several hundred vortex spacings. Nonlocal vortex flow in our experiments is observed at distances up to  $\approx 5 \mu\text{m}$ , provided a superconducting channel contains only one or two vortex rows. To the best of our knowledge, such nonlocality has neither been observed nor considered theoretically.

Our starting samples were thin films of amorphous superconductor MoGe ( $\kappa \approx 60$ ) with various thicknesses  $d$  from 50 to 200 nm. We have chosen amorphous films because they are known for their quality and very low pinning and have been extensively studied in the past in terms of pinning and vortex flow (see, e.g., [10,11]). The sharp superconducting transitions ( $< 0.1$  K) measured on mm-sized samples of our films indicate their high quality and homogeneity. The critical current  $j_C$  in intermediate fields  $b = H/H_{c2} \approx 0.3\text{--}0.6$  was measured to be  $\approx 10^2$  A/cm<sup>2</sup> (at 5 K), where  $H$  is the applied field and  $H_{c2}$  the upper critical field.  $j_C$  increased several times at lower temperatures. The MoGe films were patterned into multiterminal submicron wires of various widths  $w$  (between 70 nm and  $2 \mu\text{m}$ ) and lengths  $L$  (between 0.5 and  $12 \mu\text{m}$ ) using  $e$ -beam lithography and dry etching (see Fig. 1). Electrical measurements were carried out using the standard low-frequency (3 to 300 Hz) lock-in technique at temperatures  $T$  down to 0.3 K. The results were independent of frequency, which proves that the measured ac signals are just the same as if one were using a dc measurement technique, provided the latter could allow the same sensitivity ( $< 1$  nV). The external field  $H$  was applied perpendicular to the structured films. For brevity, we focus below on the results obtained in the nonlocal geometry and omit discussions of the complementary measurements carried out in the standard (local) four-probe geometry.

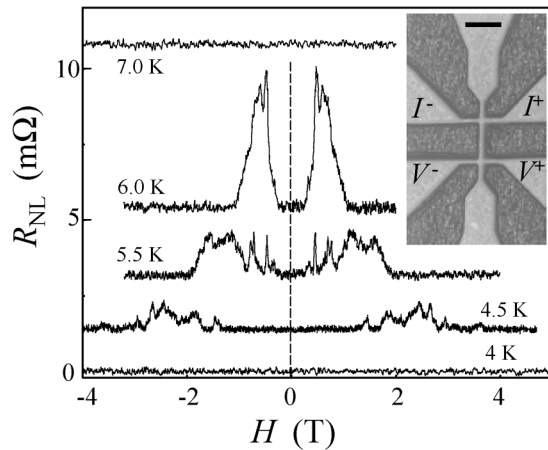


FIG. 1. Nonlocal resistance  $R_{NL}$  as a function of applied field  $H$  measured on a 150 nm wide wire at a distance of 1  $\mu\text{m}$  between the current and voltage leads. Different curves are shifted vertically for clarity ( $R_{NL}$  is always zero in the normal state). The inset shows an AFM image of the studied sample. The vertical wire in this image is referred to as central wire. Scale bar, 1  $\mu\text{m}$ .

The nonlocal geometry is explained in Fig. 1. Here, the electric current is passed through leads marked  $I^+$  and  $I^-$  and voltage is measured at terminals  $V^+$  and  $V^-$ . In this geometry, the portion of applied current  $I$  that goes sideways along the central wire (see Fig. 1) and reaches the area between the voltage probes is negligibly small. Indeed, in both normal and superconducting states [12], the current along the central wire decays as  $\propto I \cdot \exp(-\pi x/w)$ , which means that the current density reduces by a factor of 10 already at distances  $x \approx w$  and, typically, by  $10^{10}$  in the nonlocal region ( $x = L$ ) in our experiments. This also means that all vortices in the central wire, except for one or two nearest to the current-carrying wire, experience the current density many orders of magnitude below the critical value. Therefore, no voltage can be expected to be observable in the nonlocal geometry. In stark contrast, our measurements revealed a pronounced nonlocal voltage  $V_{NL}$ , which emerged just below [13] the critical temperature  $T_C$  and persisted deep into the superconducting state (Fig. 1).

The signal appeared above a certain value of  $H \approx 0.2H_{c2}$ , reached its maximum at  $(0.5-0.7) \cdot H_{c2}$  and then gradually disappeared as  $H$  approached  $H_{c2}$ .  $V_{NL}$  was found to depend linearly on  $I$  that was varied between 0.2 and 5  $\mu\text{A}$ . At lower  $I$ ,  $V_{NL}$  became so small ( $< 100$  pV) that it disappeared under noise, while higher currents led to heating effects. The linear dependence allows us to present the results in terms of resistance  $R_{NL} = V_{NL}/I$ . With increasing  $L$ ,  $R_{NL}$  was found to decay relatively slowly (for  $L \leq 4 \mu\text{m}$ ) and quickly disappeared for longer wires as well as for the wide ones ( $w \geq 0.5 \mu\text{m}$ ) (Fig. 2). The general shape of  $R_{NL}(H)$  curves was identical for all samples but fluctuations (sharp peaks) seen in Fig. 1 varied from sample to

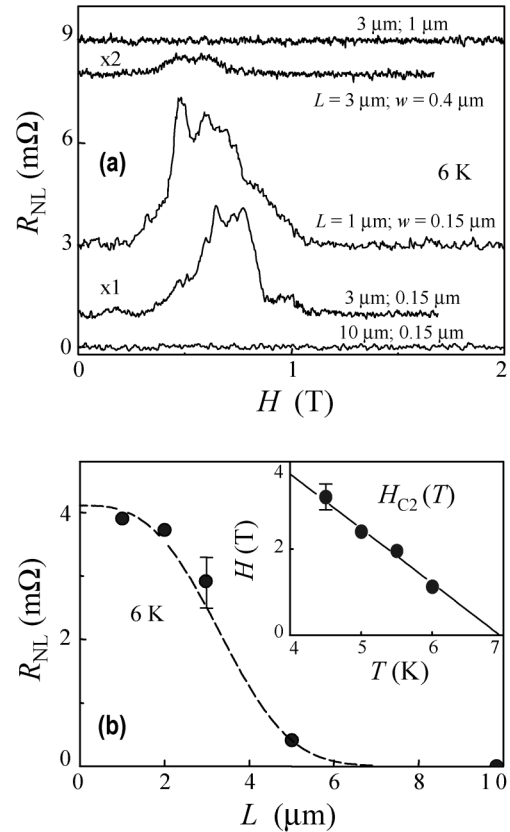


FIG. 2. Dependence of  $R_{NL}$  on length  $L$  and width  $w$  of the central wire. (a) Nonlocal resistance at  $T = 6.0$  K for different wires (their  $L$  and  $w$  values are shown on the graph). Curves are shifted vertically for clarity. (b) Nonlocal resistance at its maximum value as a function of  $L$  ( $w = 150$  nm). The signal at 6.0 K is also representative of the behavior observed at lower  $T$ . The dashed line is a guide to the eye. The inset shows temperature dependence of the field corresponding to the disappearance of  $R_{NL}$  (solid circles). The solid line is  $H_{c2}(T)$  measured on macroscopic films.

sample. A closer inspection of the fluctuations for different samples shows that they have the same characteristic interval of magnetic field over which  $R_{NL}$  changes rapidly. This correlation field  $B_C$  corresponds to the entry of one flux quantum  $\Phi_0$  into the area  $L \cdot w$  between the current and voltage leads, so that  $B_C \approx \Phi_0/L \cdot w$ .

To understand the nonlocal signal, we note that within the accessible range of  $I$ , its density inside the current-carrying wire was in the range of  $\approx 10^3$  to  $10^5$  A/cm<sup>2</sup> (i.e.,  $\gg j_c$ ) and, accordingly, caused a vortex flow through this wire. Indeed, whenever  $V_{NL}$  was observed, measurements in the local geometry showed the behavior typical for the flux flow regime. This indicates that the nonlocal resistance is related to the vortex flow in the current-carrying part of the structures, which then somehow propagates along the central wire to the region between  $V^+$  and  $V^-$  terminals, where no electric current is applied. The mechanism of the propagation can be understood as follows. The Lorentz force—acting on

vortices located at the intersection between current-carrying and central wires—pushes/pulls them along the central wire. In the absence of edge defects along this wire, the surface barrier prevents these vortices from leaving a superconductor [14] and, hence, the local distortion of the VL can be expected to propagate along the central wire, away from the current-carrying region. If the vortex motion reaches the remote intersection between the central and voltage wires, a voltage is generated by vortices passing through this region. For an infinitely rigid VL, such a local distortion would propagate any distance. However, for a soft VL and in the presence of disorder, the lattice can be compressed and vortices become jammed at pinning sites. The softer the lattice, the shorter the distance over which the distortion is dampened. Note that, as we discuss a dc phenomenon, there should exist a constant flow of vortices through the sample. We believe that this is ensured by large contact regions that act as vortex reservoirs.

The interplay between pinning and VLs elasticity is important in many vortex phenomena, and the spatial scale, over which a VL behaves as almost rigid (responds collectively), is usually determined by the correlation length  $R_C$  [15,16]. This concept had been successfully used in the past to explain the behavior of  $j_C$  in macroscopic thin films, where the only relevant elastic modulus defining  $R_C$  is the shear modulus  $C_{66}$  [17,18]. For our particular films, the maximum value of  $R_C$  can be estimated as  $\approx 20a_0$  (reached at  $\approx 0.3H_{c2}$ ) and then  $R_C$  gradually reduces to  $\approx a_0$  as  $H$  approaches  $H_{c2}$  (here,  $a_0 \approx (\Phi_0/B)^{1/2}$  is the VL period and  $B$  the magnetic induction) [10,19]. This length scale is in agreement with predictions [6,7] and clearly too short to explain the observed  $R_{NL}$ . For example, at 4.5 K,  $R_{NL}$  was detected at distances up to  $5 \mu\text{m}$  and in fields up to 3.5 T. This means that the entire vortex ensemble between the current and voltage wires, which is over 200 vortices long, is set in motion by a localized current.

To explain these unexpectedly long-range correlations, we argue that the VL in mesoscopic wires is much more rigid than in macroscopic films due to its 1D character and the presence of the edge confinement that prevents transverse vortex displacements. Indeed, if there are only a few vortex rows in a narrow channel, the only possible deformation of the lattice is via uniaxial compression. This deformation is described by compressional modulus  $C_{11} \gg C_{66}$ . In this case, the characteristic length, over which one should expect collective response, is much longer and given by another correlation length  $\lambda_C = (C_{11}/\alpha_L)^{1/2}$ , where  $\alpha_L \approx F_p/r_p$  is a characteristic of the pinning strength,  $F_p = j_C \cdot B$  the bulk pinning force, and  $r_p$  the pinning range ( $r_p \approx a_0/2$  for  $b > 0.2$ ) [2,20,21].

To calculate  $\lambda_C(H)$  we used the expression  $C_{11} \approx \Phi_0 \cdot B / (2 \cdot \mu_0 \cdot \lambda^2 \cdot a_0 \cdot k)$  expected for a 1D channel [22]. Here,  $\lambda$  is the field- and temperature-dependent penetra-

tion depth [22,23] and  $k$  the wave vector of VL deformation. Our numerical simulations show that the most relevant  $k$  is given by VLs distortion in the cross-shaped regions [see Fig. 3(b)] and, accordingly, we assume  $k \approx 1/w$ . The estimated  $\lambda_C$  in intermediate fields at  $T = 6 \text{ K}$  is  $\approx 3\text{--}10 \mu\text{m}$ , in agreement with our experiment. The above model also describes well the observed field dependences of  $R_{NL}$ . The theory curve in Fig. 3(a) takes into account that the nonlocal signal should decay as  $R_{NL} \propto \exp(-L/\lambda_C)$  where  $\lambda_C = (\Phi_0 \cdot w)^{1/2} / 2\lambda(\mu_0 \cdot j_C)^{1/2}$  and that, for narrow wires, it is thermodynamically unfavorable for vortices to penetrate the narrow wires until  $H$  reaches a critical value  $H_S \approx \Phi_0 / \pi \xi w$ . The latter effect is modeled by pinning at the surface barrier, which results in an additional part in  $j_C \propto \exp(-H/H_S)$ . The disappearance of  $R_{NL}$  below 4 K is attributed to higher  $j_C$  at lower  $T$ . Note that the exponential dependence implies that changes in  $j_C$  by a factor of 4, which occur below 5 K, result in a rapid suppression of  $R_{NL}$ .

It is clear that the above description applies only to wires that accommodate just a few vortex rows. As the number of rows increases, the VL gains an additional

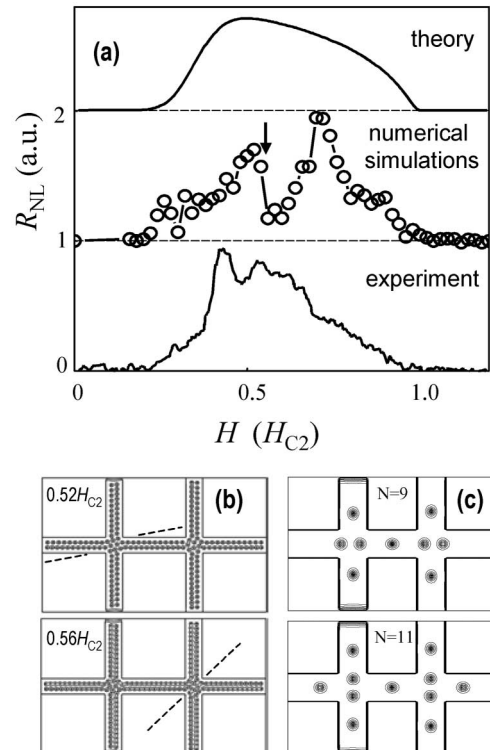


FIG. 3. (a) Comparison of  $R_{NL}(H)$  observed experimentally (lower curve; data of Fig. 1 at 6 K) with the nonlocal signal expected in the proposed 1D model (upper curve) and with results of our numerical analysis (middle curve). (b),(c) Snapshots of vortex configurations corresponding to pronounced changes in mobility of 1D vortex matter. Dashed lines indicate the average orientation of vortex rows in the cross areas.

(lateral) degree of freedom and a local compression becomes dampened by both longitudinal and lateral deformations. One eventually expects a transition to the 2D case described by the shear modulus  $C_{66}$  and a much shorter correlation length  $R_C$ . In addition, as more vortex rows are added, elastic correlations are expected to become less relevant, as vortex dynamics becomes dominated by VLs plastic deformation [22]. The latter is forbidden in a 1D case but in wider channels it can become a dominant mechanism for dampening of collective flow. This qualitatively explains the disappearance of  $R_{NL}$  in wider wires.

To support the discussed model further, we carried out direct numerical simulations of nonlocal vortex traffic, using time-dependent GL equations. The middle curve in Fig. 3(a) plots a typical example of the obtained field dependence of  $R_{NL}$  for the geometry shown in Fig. 3(b). One can see that the GL simulations reproduce the overall shape of  $R_{NL}(H)$  observed experimentally. Furthermore, the numerical analysis allowed us to clarify the origin of fluctuations in  $R_{NL}(H)$ : they appear due to sudden changes in vortex configurations. Figure 3(b) shows such changes for the field marked by the arrow in Fig. 3(a), where a sharp fall in  $R_{NL}$  is observed. Here, approximately two additional vortices enter the central wire, which results in a transition from an easy-flow vortex configuration ( $H = 0.52H_{c2}$ ) to a blocked one ( $0.56H_{c2}$ ). In the latter case, vortices in the cross-shaped regions are distributed rather randomly and break down the continuity of the vortex rows formed in the central wire. This leads to blockage of collective vortex motion. For  $H = 0.52H_{c2}$ , vortices in the cross' areas are more equally spaced, and the corresponding vortex rows make a shallower angle with rows in the central wire [Fig. 3(b)]. In this case, there is less impediment to vortex motion through the cross regions which leads to a larger nonlocal voltage.

The mechanism of the sudden blocking/unblocking of vortex flow at different  $H$  becomes even clearer if one considers an imaginary configuration containing just a few vortices—see Fig. 3(c). Here, we find a sharp fall in  $R_{NL}$  when the number of vortices changes from 9 to 11 ( $N = 10$  is a thermodynamically unstable state for this geometry). For  $N = 9$ , the vortex row passes continuously through the whole central wire, allowing its motion as a whole when pushed or pulled along by a localized current. In contrast, for  $N = 11$ , there is a vortex pair in each of the crosses which prevents such vortex motion.

In conclusion, we have observed pronounced flux flow at distances corresponding to hundreds of VL periods from the region where applied current flows. We attribute the observed behavior to an enhanced rigidity of the

vortex lattice confined in narrow channels and provide a theoretical model for this.

We thank M. Blamire, M. Moore, and V. Falko for helpful discussions.

- 
- [1] G. Blatter *et al.*, *Rev. Mod. Phys.* **66**, 1125 (1994).
  - [2] E. H. Brandt, *Rep. Prog. Phys.* **58**, 1465 (1995).
  - [3] I. Giaever, *Phys. Rev. Lett.* **15**, 825 (1965).
  - [4] R. Busch *et al.*, *Phys. Rev. Lett.* **69**, 522 (1992); H. Safar *et al.*, *Phys. Rev. B* **46**, 14 238 (1992).
  - [5] J. W. Ekin, B. Serin, and J. R. Clem, *Phys. Rev. B* **9**, 912 (1974).
  - [6] M. C. Marchetti and D. R. Nelson, *Phys. Rev. B* **42**, 9938 (1990).
  - [7] R. Wortis and D. A. Huse, *Phys. Rev. B* **54**, 12 413 (1996); S. J. Phillipson, M. A. Moore, and T. Blum, *Phys. Rev. B* **57**, 5512 (1998).
  - [8] D. López *et al.*, *Phys. Rev. Lett.* **82**, 1277 (1999).
  - [9] Yu. Eltsev *et al.*, *Physica (Amsterdam)* **341C–348C**, 1107 (2000); J. H. S. Torres *et al.*, *Solid State Commun.* **125**, 11 (2003).
  - [10] P. H. Kes and C. C. Tsuei, *Phys. Rev. B* **28**, 5126 (1983); R. Wördenweber and P. H. Kes, *ibid.* **34**, 494 (1986).
  - [11] A. Pruyboom *et al.*, *Phys. Rev. Lett.* **60**, 1430 (1988); N. Kokubo *et al.*, *Phys. Rev. Lett.* **88**, 247004 (2002).
  - [12] The dependence  $\exp(-\pi x/w)$  follows directly from the formalism introduced by L. J. van der Pauw, *Philips Tech. Rev.* **20**, 220 (1958). We have also validated this formula for the zero resistance state through numerical simulations using GL equations.
  - [13] Very close to  $T_C$ , we observed a nonlocal effect of another origin. This signal exhibits a different shape and different  $L$  and  $w$  dependences (e.g., it could be detected for any  $w$  but only for  $L \leq 2 \mu\text{m}$ ). We attribute the near- $T_C$  signal to quantum interference corrections to conductivity [L. I. Glazman *et al.*, *Phys. Rev. B* **46**, 9074 (1992)].
  - [14] L. Burlachkov, *Phys. Rev. B* **47**, 8056 (1993).
  - [15] A. I. Larkin and Yu. N. Ovchinnikov, *J. Low Temp. Phys.* **34**, 409 (1979).
  - [16] H. R. Kerchner, *J. Low Temp. Phys.* **50**, 337 (1983).
  - [17] P. H. Kes and C. C. Tsuei, *Phys. Rev. Lett.* **47**, 1930 (1981).
  - [18] E. H. Brandt, *Phys. Rev. Lett.* **50**, 1599 (1983); *J. Low Temp. Phys.* **53**, 71 (1983).
  - [19] N. Toyota *et al.*, *J. Low Temp. Phys.* **55**, 393 (1984); J. Osquiguil, V. L. P. Frank, and F. de La Cruz, *Solid State Commun.* **55**, 222 (1985).
  - [20] A. M. Campbell, *J. Phys. C* **2**, 1492 (1969); **4**, 3186 (1971).
  - [21] E. H. Brandt, *Phys. Rev. Lett.* **67**, 2219 (1991).
  - [22] R. Besseling *et al.*, *Europhys. Lett.* **62**, 419 (2003).
  - [23] E. H. Brandt, *J. Low Temp. Phys.* **26**, 709 (1977); **26**, 735 (1977).